Spectrum-Sculpting-Aided PU-Claiming in OFDMA Cognitive Radio Networks

Yi Ren(✉), Chao Wang, Dong Liu, Fuqiang Liu, and Erwu Liu

School of Electronic and Information Engineering, Tongji Uniniversity, Shanghai, People's Republic of China
{092755,chaowang}@tongji.edu.cn,
liu-dong@live.cn, liufuqiang@tongji.edu.cn, erwu.liu@ieee.org

Abstract. We consider a cognitive radio network where the primary user (PU) supports applications with multiple quality of service (QoS) requirements via orthogonal frequency division multiple access (OFDMA). To let the secondary users (SUs) be aware of PU's QoS level, and hence provide PU with sufficient protection, we propose a spectrum-sculpting-aided PU-claiming scheme that does not demand strict PU-SU synchronization. Specifically, the PU deliberately inserts one zero-subcarrier into its subcarriers, the position of which represents the QoS requirement of the PU. Through a two-step sensing procedure, each SU then can estimate the QoS requirement and adjust its sensing or accessing strategies accordingly. Simulation results exhibit the advantages of the proposed scheme, in terms of both weighted received interference (WRI) and SU's throughput[1].

Keywords: Spectrum sculpting · Cognitive radio · Multi-QoS · OFDM · PU-claiming

1 Introduction

The explosive increase of wireless devices and services in recent years will potentially lead to a scarcity in spectrum resource. On the other hand, as reported by FCC, the conventional fixed spectrum allocation policy results in a heavy spectrum underutilization, which exacerbates the shortage of spectrum resource. In order to handle this issue, the concept of cognitive radio (CR), which gives secondary users (SUs) the ability to probe and access specific spectrum bands when they are not occupied by primary users (PUs), has been proposed and studied intensively [1].

Previously, most works on spectrum sensing and accessing mainly assume that PU only has one quality-of-service (QoS) level, hence the SU usually has a constant configuration in terms of detection probability or power constraints.

This work was supported in part by the Key Program of National Natural Science Foundation of China under Grant No. 61331009 and the Fundamental Research Funds for the Central Universities No. 0800219236.

M. Weichold et al. (Eds.): CROWNCOM 2015, LNICST 156, pp. 295–307, 2015.
DOI: 10.1007/978-3-319-24540-9_24

However, multi-QoS system is also an important scenario, especially when some modern wireless communication systems (e.g. LTE or WiMAX [2]) which have large amount subscribed users are considered as PU. In this paper we consider a more complex primary network which will have applications with different QoS requirement levels, and these distinct applications will be dynamically served in PU's allocated bands. Under such condition, the constant constraints for SU may be not satisfactory. For instance, for some delay-sensitive or real-time applications, even small interference caused by SU brings enormous economic cost, while many data-service applications such as email and downloading can tolerate more interference. Thus in multi-QoS systems, the sensing strategies of SU should be adaptive according to PU's QoS requirements to provide a better protection for PU, and potentially, increase its own throughput. Enabling information sharing between PU and SU (we call this *PU-claiming*) may be an effective way to realize such an adaptation. However, as primary network and secondary network are usually heterogeneous, and also because PU's signal is usually weak at SUs, such PU-claiming may be hard to realize. Conventionally, some researches assume that PU can periodically broadcast beacon-frames to SUs to deliver some important information to SUs (as mentioned in [3], [4] and [5]). However, such beacon-based PU-claiming scheme faces three practical roadblocks: the conundrum of strict synchronization between PU and SU; sometimes, PU's weak signal power at SU and the considerable resource squander of PU.

To address these problems, in this paper we propose a spectrum-sculpting-aided PU-claiming scheme for orthogonal frequency division multiple access (OFDMA) systems. Specifically, inspired by spectrum notching [6], which has been intensively discussed in NC-OFDM (non-continuous OFDM) systems for interference controlling, we require the PU to deliberately insert one zero-subcarrier (named as *spectrum valley*) into its subcarriers of each service. The position of the spectrum valley is used to represent the QoS requirement. When each SU conducts a two-step spectrum sensing and attains such information, it can adjust its sensing parameters accordingly to provide corresponding protection to the PU. Since the QoS requirements of PU's applications are inherently attached in the spectrum structure and can be changed dynamically, a strict synchronization between PU and SUs is not necessary (i.e. SU can attain such information no matter when it intends to conduct spectrum sensing). Through mathematical analysis and numerical simulations, we show that the proposed scheme brings a significant performance improvement in terms of *weighted received interference* (WRI) over the conventional scheme proposed in[7]. And from SU's perspective, SUs with PU-claiming can also have potential to gain a higher throughput even through PU may possibly have some extremely interference-sensitive applications.

2 System Description

2.1 System Model

We consider a CR-OFDMA system with one centralized primary network (e.g., LTE systems). The PU's base station (BS) uses N_B frequency channels tosupport diverse services, such as voice, data traffic and real-time applications, to its subscribed users. Fig.1-A illustrates a typical frequency-domain structure of LTE signal. The entire band of N_f adjacent subcarriers is divided into N_B channels, each containing L'_d subcarriers. Several unused subcarriers, termed *virtual carrier (VC)*, locate at the edges of the band to avoid energy leakage. The PU's transmitting signal is expressed as

$$s_i(t) = \frac{1}{N_f} \sum_{n=0}^{N_f-1} S_i(n) G(n) e^{\frac{j2\pi nt}{N_f}}, \quad t \in \{0, \cdots, N_f - 1\}, \tag{1}$$

where N_f is the symbol size, and $S_i(n)$ is the frequency-domain transmitted signal at the nth subcarrier in the ith symbol. $G(n)$, called *transmitted kernel function*, represents the spectrum structure of OFDM signal, is set to be 1 if the nth subcarrier is occupied by a PU application, and be 0 otherwise. To simplify analysis, the processes of adding cyclic prefix and windowing are not considered, because they have no influence on the frequency-domain structure of PU's signal.

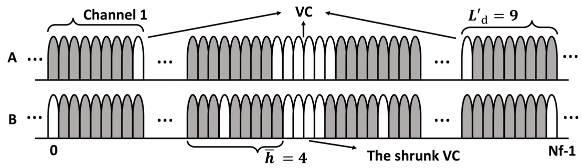

Fig. 1. Spectrum sculpting of PU's transmitted OFDM signal

An SU locating in the vicinity of PU is allowed to conduct spectrum sensing and opportunistically access the channels that are not occupied by PU. Constrained by sampling rate, each SU can perform sensing on only one channel at a time instant. Due to SU's imperfect spectrum sensing, PU will inevitably be interfered if any SU mistakenly treats an occupied channel as unused. Clearly, applications with higher QoS requirements are more sensitive to such interference, i.e., they have higher cost compared to applications with lower QoS requirements when suffered by interference. Similar to the priority table defined in [2], we can use an integer variable $k \in \{1, 2, \cdots, K\}$ to classify those applications and represent the QoS requirement level of current application ($k = K$ denotes the most sensitive application).

2.2 Performance Metrics

The performance of the CR system can be considered from two perspectives. From PU's viewpoint, we use WRI ($\mathcal{W}$), i.e. the weighted received interference, to evaluate the impact of SUs' interference on the PU network. The WRI is defined as follows and can be used to indicate the performance cost or economical cost sacrificed by the PU for permitting SUs' access:

$$\mathcal{W} = \sum_{k=1}^{K} \omega_k \cdot I_k \cdot M_k, \tag{2}$$

where I_k denotes the interference intensity experienced by the level-k applications and ω_k is the associated weighting factor. M_k can be considered as the level-k application's cumulative operating time in the observation duration (or the probability that a level-k application may be served). Note that the value of ω_k mainly depends on the customers' requirement, which can be attained by the telecom operators via long term observing, so as the M_k. Then the SU can buy these message from the telecom operators or just learn from its history observations. Depending on the objective, there are different ways to define I_k. For instance, one can use SU's miss detection probability or the average interference power seen by the PU to serve as I_k. Generally speaking, as those applications with higher QoS requirement are usually more sensitive to SU's interference, hence the corresponding ω_k will be larger comparing with that of low level applications. Then $\mathcal{W}$ can be used to assess the performance of secondary access strategies in CR networks: the approaches applied by SU that lead to a smaller value of $\mathcal{W}$ potentially provides PU with more protection. On the other hand, we can compare the system performance from SU's perspective: satisfying PU's protection requirements level, the strategies lead to a higher throughput of SU are better. To initially show the advantages of the proposed spectrum-sculpting-aided PU-claiming scheme, in Section 5 we simply set ω_k as a linear function of k and set I_k as the statistical times of SUs' disturbance toward the PU.

3 Spectrum-Sculpting-Aided PU-claiming

As stricter protection is required by those higher-level applications while more access opportunities embed in the spectrum which serving lower-level applications, a simple way to enhance the system performance is to feed the information regarding k to SU. Armed with such knowledge, the SU can adapt its sensing and accessing strategies accordingly.

3.1 PU's Spectrum Sculpting

To establish PU-claiming more efficiently, we consider moving a VC into each channel. In other words, in the PU's signal structure, each channel now contains $L_d = L'_d + 1$ data subcarriers and one of them is a zero-subcarrier (termed *spectrum valley*). The potential locations of the spectrum valley are selected in such a way that each position can be mapped to a QoS requirement level. Without loss of generality, we assume that the first K subcarriers (assume $K \leq L_d$) in each channel are used to place the spectrum valley. Let $\bar{h} \in \{1, \cdots, K\}$ denote the position index of the spectrum valley in the signal of current application. The frequency-domain signal structure when $\bar{h} = 4$ is illustrated in Fig. 1-B. It should be noted that moving VC into the channels results in a slight reduction

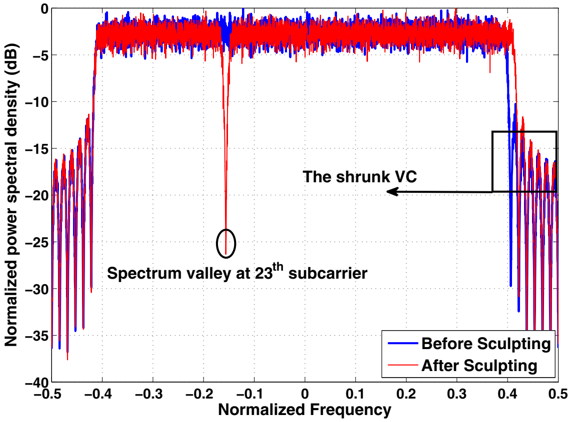

Fig. 2. Spectrum sculpting on one channel of OFDMA signal.

of the width of VC. Nevertheless, we observe that in many OFDMA systems the VC's width is not fixed but selected within a certain range (i.e. 159-183 in [8] when $N_f = 1024$). Fig.2 illustrates how PU sculpt its spectrum to make a spectrum valley. We can see the width of VC in the right side is shrunk by spectrum sculpting. Nevertheless, due to the sharp out-band decrease of one subcarrier's power spectral density, the power at the edge of this band (after sculpting) is still less than -18dB, which is almost the same comparing with the energy leakage before spectrum sculpting. In addition, some time-domain windowing techniques can effectively restrain the leakage of side-lobe [9]. And in practice, there should not always be signals transmitting in its adjacent channel. Hence the resulting energy leakage brought by the smaller VC should not be noticeable.

3.2 SU's Two-step Spectrum Sensing

Regarding SU, akin to [4], we also formulate SU's behavior by two kinds of frames: transmitting frame with the duration T_t and sleeping frame with the duration T_s. SU will conduct a *two-step spectrum sensing* to detect target channel's condition. And attain the value of k which is embedded to PU's signal structure. Particularly, the SU first applies an energy detection algorithm to determine whether this channel is occupied by the PU. Note that SU will store the data samples used for first step sensing in a samples queue (can contain totally N_Q transmitting frames) as long as the result of first-step detection is yes. Knowing the presence of PU, the SU will then detect the spectrum valley's position by searching for the subcarrier with the smallest energy among the first K subcarriers of the channel. Generally speaking, as the switches of PU's application level is far slower than the switches of PU's presence/absence status [10], the samples queue can easily store enough data samples for the second-step sensing. Since the result of this step indicates the QoS requirement level of the service currently operating in this channel, the SU adjusts its sensing parameters accordingly for the next sensing to reduce the WRI. After this, SU will step into sleeping process. Otherwise, if the detection in the first step shows that the channel is unused, the SU steps into transmitting process. To conduct the two-step spectrum sensing, the SU firstly sample the analog signals using a sampling frequency f_s, then separates data samples using an L_d-point fast Fourier transform (FFT) block. The mth output of the FFT block is:

$$Y_m(i) = \sum_{n=0}^{L_d-1} y_i[n] \cdot e^{-j\frac{2\pi mn}{L_d}} \quad m \in \{1, \cdots, L_d\}, \tag{3}$$

where $y_i[n]$ is the sampled discrete signal in time-domain, and i is the index of OFDM symbol (without considering CP). Specifically, when PU is active:

$$Y_m(i) = \sum_{t=0}^{L_d-1} (\sum_{l=0}^{L_d-1} (h(l)s_i(t-l)) + v(t))e^{-j\frac{2\pi mt}{L_d}}. \tag{4}$$

Hence we can divide the mth output of FFT block as follows:

$$\begin{array}{ll} Y_m(i) = V(n) & \text{CASE} - \text{I} \\ Y_m(i) = H(m)S_i(m) + V(n) & \text{CASE} - \text{II}, \end{array} \tag{5}$$

where $H(m)$, $S_i(m)$ and $V(n)$ are frequency-domain form of channel response, signal and noise. We assume a frequency-flat channel, i.e. $H(m) = H$ to make a initial analysis. The influence of fading channel will be left for future. In equation (5), the CASE-I represents the scenario that $\mathcal{H} = 0$ (PU not active in practice), or $\mathcal{H} = 1$ *and* $G(m) = 0$ (PU is active and the mth subcarrier is spectrum valley or VC). And the CASE-II represents that $\mathcal{H} = 1$ *and* $G(m) = 1$ (PU is active and the mth subcarrier is data carrier). Let τ be the sensing time and N_r be the number of data samples used for the first-step sensing in one frame ($N_r = \tau f_s$), the mth subcarrier's energy can be expressed as:

$$T(m) = \frac{L_d}{N_r} \sum_{i=1}^{\lfloor \frac{N_r}{L_d} \rfloor} |Y_m(i)|^2. \tag{6}$$

Assume $E[|V(t)|^2]{=}\sigma_v^2$, $E[|S_i(m)|^2]{=}\sigma_s^2$ and let $\rho{=}\frac{\sigma_s^2}{\sigma_v^2}$ represent the transmitting signal-to-noise ratio. Using the central limit theorem (CLT), the energy $T(m)$ in CASE-I and CASE-II can be approximated by Gaussian variables. Specifically, in CASE-I, $T(m) \sim \mathcal{N}(\mu_0, \sigma_0^2)$, where $\mu_0{=}\sigma_v^2$ and $\sigma_0^2{=}\frac{L_d}{N_r}\sigma_v^4$ while in CASE-II, $T(m) \sim \mathcal{N}(\mu_1, \sigma_1^2)$ where $\mu_1{=}(1 + H^2\rho)\sigma_v^2$ and $\sigma_1^2{=}\frac{L_d}{N_r}(1 + H^2\rho)^2\sigma_v^4$.

Use variable $\hat{\mathcal{H}}$ to represent the SU's detection decision. The probability that the SU correctly detects the existence of the PU when it is active (i.e. the *detection probability*) is expressed as $P_d := P_r\{\hat{\mathcal{H}} = 1|\mathcal{H} = 1\}$. Similarly, the *false alarm probability* is $P_f := P_r\{\hat{\mathcal{H}} = 1|\mathcal{H} = 0\}$. Different from the conventional energy detection algorithm that calculates sum energy in the time domain, we apply an energy detector at each SU using energy accumulated from all the subcarriers of current channel, i.e.,

$$\lambda := \frac{1}{L_d}\sum_{m=1}^{L_d} T(m) - \epsilon_k \tag{7}$$

where ϵ_k is the decision threshold knowing the level of current application is k. $\lambda > 0$ claims $\hat{\mathcal{H}} = 1$ and $\lambda < 0$ claims $\hat{\mathcal{H}} = 0$. Thanks to Parseval theorem, this frequency-domain detector leads to the same result as conventional time-domain energy detector, because this energy detector collects the energy of all the outputs (including VC and spectrum valley). Again, using CLT we can see that $\lambda_{|\mathcal{H}=1} \sim N(\bar{\mu}_1, \bar{\sigma}_1^2)$, where $\bar{\mu_1} = \mu_1$ and $\bar{\sigma}_1^2 = \frac{\sigma_1^2}{L_d}$. Similarly, $\lambda_{|\mathcal{H}=0} \sim N(\bar{\mu}_0, \bar{\sigma}_0^2)$, where $\bar{\mu_0} = \mu_0$ and $\bar{\sigma}_0^2 = \frac{\sigma_0^2}{L_d}$. Given P_d, after some mathematical manipulations, we can express P_f, which mainly influences SU's throughput, as:

$$P_f = \mathcal{Q}\left(\frac{\bar{\sigma}_1}{\bar{\sigma}_0}\mathcal{Q}^{-1}(\bar{P}_d) + \frac{\bar{\mu}_1 - \bar{\mu}_0}{\bar{\sigma}_0}\right). \tag{8}$$

where Q-function $\mathcal{Q}(\cdot)$ is complementary cumulative distribution function of standard Gaussian distribution $\mathcal{Q}(x) = \frac{1}{\sqrt{2\pi}}\int_x^{\infty} e^{-\frac{t^2}{2}}dt$.

If the above process shows the channel is currently occupied, the SU starts detecting the position of the spectrum valley, $\bar{h}$, by comparing the energy values of different subcarriers and choosing the one with the smallest energy. Using P_s to represent the probability that the SU correctly locates the spectrum valley, given that it successfully detects the existence of PU in the first step, we can have:

$$\begin{aligned} P_s &= P_r\{\hat{h} = k|\bar{h} = k\} \\ &= P_r\{\tilde{T}(k) < \tilde{T}(m),\ m \in [1,k], m \neq k\}. \end{aligned} \tag{9}$$

As the second-step sensing uses the samples stored in samples queue, which contains the samples of N_Q frames. Using CLT, we can obtain $\tilde{T}_I := \tilde{T}(m)_{|CASE-I} \sim \mathcal{N}(\tilde{\mu}_0, \tilde{\sigma}_0^2)$ and $\tilde{T}_{II} := \tilde{T}(m)_{|CASE-II} \sim \mathcal{N}(\tilde{\mu}_1, \tilde{\sigma}_1^2)$. The expectation and variance of these two cases are: $\tilde{\mu}_0 = \sigma_v^2$, $\tilde{\sigma}_0^2 = \frac{L_d}{N_Q N_r}\sigma_v^4$, $\tilde{\mu}_1 = (1 + H^2\rho)\sigma_v^2$ and $\tilde{\sigma}_1^2 = \frac{L_d}{N_Q N_r}(1 + H^2\rho)^2\sigma_v^4$. Given the probability distribution function (PDF) of $\tilde{T}(m)$ under both CASE-I and CASE-II, the equation (9) can be calculated by multiple integral. Specifically, we use $\{x_1, x_2, \ldots, x_K\}$ to represent these K random variables. Without loosing generality, we assume x_1 and $\tilde{T}_I$ have identical distribution and x_m $(m = 2, 3, \ldots, K)$ has identical distribution with $\tilde{T}_{II}$. The joint probability distribution function of these K random variables can be expressed by:$f_T(x_1, \ldots, x_K)$. Following the assumption that random variables $x_m,\ m = 2, 3, \ldots, K\}$ are identically independently distributed (i.i.d), applying the distribution of $\tilde{T}_I$ and $\widetilde{T}_{II}$, we can have:

$$f_T(x_1, \ldots, x_K) = \frac{1}{(2\pi\tilde{\sigma}_0^2)^{\frac{1}{2}}} e^{-\frac{(x_1-\tilde{\mu}_0)^2}{2\tilde{\sigma}_0^2}} \cdot \prod_{i=2}^{Q-1} \frac{1}{(2\pi\tilde{\sigma}_1^2)^{K-1}} e^{-\sum_{i=2}^{K-1}\frac{(x_i-\tilde{\mu}_1)^2}{2\tilde{\sigma}_1^2}}. \tag{10}$$

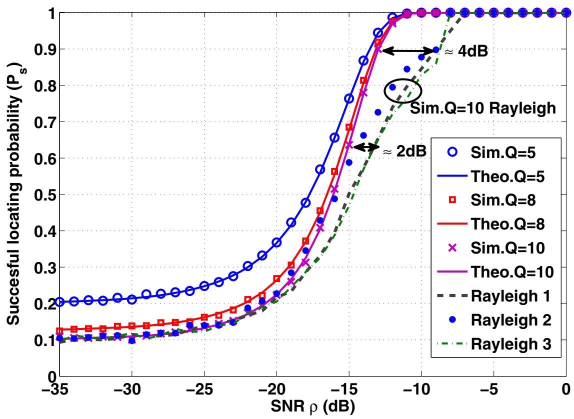

Fig. 3. Probability of successfully location the spectrum valley.

Then P_s can be expressed as:

$$P_s = \int_{\mathbb{R}^{\mathbb{T}}} f_T(x_1, \ldots, x_K) dx_1 dx_2 \ldots dx_K, \tag{11}$$

where $\mathbb{R}^{\mathbb{T}}$ is the field of integration in which $\{x_1 < x_m,\ m = 2, 3, \ldots, K]\}$ will hold (i.e. $\mathbb{R}^{\mathbb{T}} = \bigcap_{m=2}^{K}\{x_1 < x_m\}$). Hence the equation (11) can be decomposed as:

$$P_s = \int_{-\infty}^{\infty} \int_{a}^{\infty} \cdots \int_{a}^{\infty} f_T(x_1, \ldots, x_K) dx_K \ldots dx_2 dx_1. \tag{12}$$

Finally, substituting equation (10) and Q-function to equation (12), the P_s can be estimated as:

$$P_s = \int_{-\infty}^{\infty} \frac{1}{\sqrt{2\pi}\tilde{\sigma}_0} e^{-\frac{(a-\tilde{\mu}_0)^2}{2\tilde{\sigma}_0^2}} \mathcal{Q}^{K-1}\left(\frac{a - \tilde{\mu}_1}{\tilde{\sigma}_1}\right) da. \tag{13}$$

Additionally, the probability that the SU wrongly claims the spectrum valley's position as $\hat{h} = l$ (when in practice, $\bar{h} = k$) is represented by $P_e := P_r\{\hat{h} = l, l \neq k|\bar{h} = k\} = \frac{1-P_s}{K-1}$, because the energy of all the data subcarriers' are identically independently distributed (i.i.d). Fig.3 illustrates the simulation results and mathematical approach of analyzing the probability of successfully locating the spectrum valley (N_f=64 and 20000 data samples are used). From Fig.3, we can see the simulation results fit the estimation well, and the value of P_s converges to one when SNR is large while it converges to $\frac{1}{K}$ when SNR is low. In other words, P_s will be always no less than P_e, and the worst case is that SU randomly selects a position from the L_d potential subcarriers. Considering the influence of fading on our proposed scheme, we simulated the signal experienced three different Rayleigh fading channels. Specifically, the channel named Rayleigh 1 has 6 taps ([0 -8 -17 -27 -25 -31]dB), and the delay of these factor is [0 4 8 12 16 20]; Rayleigh 2 has same taps with Rayleigh 1, but the delay factor changes to [0 1 2 3 4 5]; Rayleigh 3 only has 4 taps ([0 -8 -17 -27]dB) and the delay vector is [0 4 8 12]. Comparing Rayleigh 1 and 2, we can see the larger the delay factor is, the worse the P_s is, which coincides with our intuition that larger time-domain spread will harm the detection performance more. Comparing Rayleigh 1 and 3, we find that the performance does not change so much. That is because the first 4 taps of Rayleigh 3 and 1 are the same. The gap between P_s under AWGN and Rayleigh 1 channel ranges from zero to approximately 4dB, and larger gap exists when SNR is small.

3.3 Weakness Discussion

Comparing with conventional beacon based PU-claiming schemes, the proposed method can skillfully solve some conundrums such as synchronization, high dynamic and low received power. However, this scheme inherently has its short comings. First, the specific squander and sacrifice of PU is hard to qualified. Because moving one VC will keep the spectrum efficiency of the PU in target channel constant, however, the shrunk VC will cause interference to adjacent channels. Second, this scheme need to be optimized to compete with more serious fading scenarios. Which will be left for our future work.

4 Performance Analysis

Knowing the position of the spectrum valley, the SU is able to attain the level of current application, and thus the knowledge of ω_k and $\bar{I}_k$ (here we use $\bar{I}_k$ to represent the requirement of PU's level-k application) from a pre-defined table in standards or protocols. Then, SU can adjust its sensing and transmission strategies accordingly to avoid causing a large $\mathcal{W}$ and improve its throughput under PU's constraints. Assume I_k is the interference probability observed at PU, then SU must set appropriate P_d^k to ensure $I_k \leq \bar{I}_k$. On the other hand, as the interference intensity is defined as *SU's miss detection probability* in this paper, the relationship between P_d^k and I_k can be expressed as follows:

$$1 - I_k = P_s P_d^k + P_e \sum_{l=1, l \neq k}^{K} P_d^l, \tag{14}$$

which means that the interference caused by the SU applying our scheme to the level-k application can be divided into K sub-conditions: one is the SU correctly detect the level-k application being served while another $K-1$ are the scenario that SU wrongly claims a level-l application as level-k.

In this paper, three different kinds of SUs are considered: 1) *no PU-claiming (NC)*: SU does not know PU's QoS level and choose a constant P_d for all applications; 2) our *spectrum-sculpting-aided PU-claiming (SC)* and 3) *genie-aided PU-claiming (GC)*: SU perfectly knows PU's exact QoS level, which can be considered as the extreme scenario for SC that $P_s \rightarrow 1$. Note that NC-SU and GC-SU will just have $I_k = 1 - P_d^k$.

Table 1. Performance of 3 WRI with 50000 sec. observation.

	WRI				Comparison (%)	
	SC	GC	NC	Mth.	GC/NC	SC/GC
A	66.413	62.578	86.665	65.667	72.22	106.1
B	54.404	51.193	73.008	53.208	70.12	106.2
C	29.665	28.056	40.807	29.254	68.75	105.7

Firstly, we will observe the system performance from PU's perspective, i.e. the value of weighted received interference defined in equation (2). To calculate I_k, we observe one channel for a duration T_c (assumed to be sufficiently large), within which only one type of application is served. The probability that PU occupies the channel is denoted by $\mathcal{P}_1 = P_r\{\mathcal{H} = 1\}$. Use D_{01} and D_{11} to represent the numbers of times that the events $\{\hat{\mathcal{H}} = 0|\mathcal{H} = 1\}$ and $\{\hat{\mathcal{H}} = 1|\mathcal{H} = 1\}$ occur within the duration T_c, respectively. We have:

$$\begin{aligned} &\tfrac{D_{11}}{D_{01}+D_{11}} = P_d^k \\ &T_t D_{01} + T_s D_{11} = T_c \mathcal{P}_1. \end{aligned} \tag{15}$$

When PU is active, SU's miss detection causes interference. Using the above relations, I_k can be expressed as:

$$I_k := \frac{D_{01}}{T_c} = \frac{(1-P_d^k)\mathcal{P}_1}{T_t(1-P_d^k) + T_s P_d^k}. \tag{16}$$

Secondly, from SU's perspective, we can assume PU is strict and requires all the level of its applications should be well protected, i.e., SU must ensure $I_k \leq \bar{I}_k$, $\forall k$. Under such condition, NC-SU have to choose $P_d = 1 - \min(\bar{I}_k)$, $\forall k$, and SC-SU must apply equation (14) to PU's constraints to calculate the according P_d^k. Then, similar with the process of analyzing SU's interference, we use D_{00} and D_{10} to represent the numbers of times that the events $\{\hat{\mathcal{H}} = 0|\mathcal{H} = 0\}$ and $\{\hat{\mathcal{H}} = 1|\mathcal{H} = 0\}$ occur within the duration T_c, respectively:

$$\begin{aligned} &\tfrac{D_{10}}{D_{00}+D_{10}} = P_f^k \\ &T_t D_{00} + T_s D_{10} = T_c(1-\mathcal{P}_1), \end{aligned} \tag{17}$$

where P_f^k is calculated by applying P_d^k to equation (8). Then, using R_0 to represent SU's data rate and by solving the equation set (17), the SU's throughput can be expressed as:

$$\mathcal{C} = \sum_{k=1}^{K} M_k \Big(\frac{D_{00}(T_t - \tau)R_0}{T_c T_t}\Big) = \frac{(T_t-\tau)R_0}{T_t} \sum_{k=1}^{K} M_k \frac{(1-\mathcal{P}_1)(1-P_f^k)}{T_t(1-P_f^k) + T_s P_f^k}. \tag{18}$$

5 Simulations and Comparisons

In this section, numerical simulations are conducted to evaluate the enhancement of our proposed scheme from both PU's perspective (compare WRI) and SU's

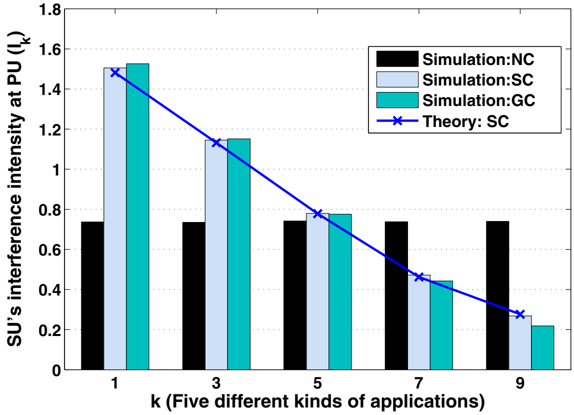

Fig. 4. Average I_k under 50000 seconds simulation, when k=1, 3, 5, 7, 9

perspective (compare throughput). We employ Monte-Carlo simulations, which observe one SU's access behavior in a centralized PU network for 50000 seconds. We set N_f=1024, K=10, L'_d=48, N_B=30, f_s=20MHz, τ=2ms, SNR=-12.5dB, T_t=200ms, $M_k|_{\forall k}$=$\frac{1}{K}$ and $\mathcal{P}_1$=0.5.

Firstly, we compare the value of $\mathcal{W}$ when all SUs throughput are equal. To calculate the WRI, we consider a simple example that the detection probability at SU is a linear function of k, i.e., $\bar{I}_k = \frac{1.99}{9} - \frac{0.19}{9}k$ which results in $\bar{I}_1$=0.2 and $\bar{I}_{10}$=0.01. In addition, simply let $\omega_k = k$.

Table 1 compares the WRI of the simulation results of the three schemes and SC-SU's mathematical estimation based on (16). Three different sleeping frame lengths are considered: A (T_s=10ms), B (T_s=20ms), and C (T_s=40ms). Intuitively, SU with larger T_s conducts spectrum sensing more infrequently, and thus has less chances to interfere the PU. From the first four columns, we can see that $\mathcal{W}$ reduces by increasing T_s in each scheme. The column "GC/NC" shows the improvement of $\mathcal{W}$ when PU-claiming introduced to the system, while "SC/GC" shows the gap between actual condition and ideal condition. Clearly, the estimation error of the spectrum valley's position does not significantly reduce the performance of the proposed PU-claiming scheme. Fig.4 depicts the I_k of five different types of applications with k=1, 3, 5, 7, 9 when T_s=40ms. We assume that in the NC scheme the SU conducts spectrum sensing with a fixed detection probability since it does not know the PU's QoS requirement. Hence in different applications, it introduces interference to the PU with a stable frequency. From the figure we can see that using PU-claiming, the frequency that SU introduces interference to PU depends on the QoS requirement level. By this means, the protection provided to PU and the opportunities provided for SU can be much better balanced. Again, since the performances of the GC and SC schemes are close, estimation error at the second detection step does not have obvious impact to the system performance. Finally, simulation results coincide with mathematical analysis. The advantages of the proposed scheme are clearly exhibited.

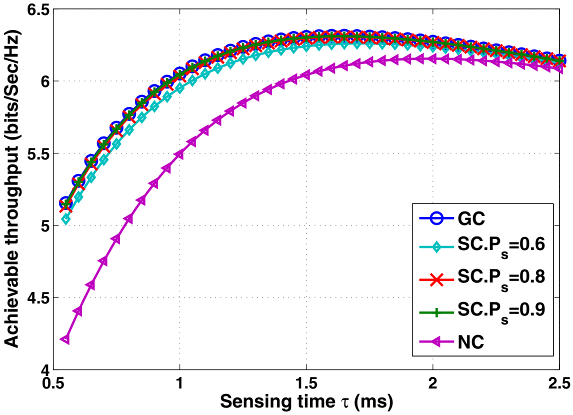

Fig. 5. Comparison of achievable throughput of different kinds of SUs.

Then, we consider a scenario that PU is strict, in which SUs must ensure all PU's applications are satisfied. Regarding SC-SU, for a given P_s, it must apply equation (14) to PU's constraints ($I_k \leq \bar{I}_k$), then use the calculated P_d^k to sense and access, and use the corresponding P_f^k to estimate SU's throughput. Similar with previous simulation, we set $R_0 = 10$ and observe the influence of τ. Assume $K = 6$ and M_k has a Gaussian distribution. To make an initial analysis, we compare the scenario that P_s does not vary with sensing time τ. Note that the value of P_s can be ensured by extending the length of the samples queue (N_Q). In Fig.5, the throughput of these three kinds of SUs are compared. NC-SU must ensure the most sensitive application, hence it has the worst performance. Knowing the knowledge of current application, we see the throughput will have a significant improvement. In this figure, there is a tradeoff between SU's sensing time τ and its achievable throughput: The throughput firstly increases when sensing time τ becomes larger, that is because longer τ implies more data samples used for energy detection. However, too long sensing time will shrink the time of SU's data delivery, which in turn lead the achievable throughput decreases. Another interest thing illustrated in this figure is that, we see when P_s is larger than 0.8, the performance of SC-SU is already very close to that of GC-SU, when P_s equal 0.9, their curves almost coincide. That is to say under some conditions, P_s has no need to be so closed to one (say 0.999).

6 Conclusion

Considering the fact that different PU applications may have different QoS requirements in modern wireless communication systems, we established PU-claiming to share the QoS level between PU and SU. With the help of such knowledge, SUs should adjust their transmission and sensing strategies to provide sufficient protection to the PU. To provide the SUs with the QoS requirements, we use a spectrum sculpting techniques to create a specific spectrum valley in each PU application's data frame. Via a two-step sensing procedure, the SU estimates the spectrum valley's position if it determines that the interested channel is occupied by PU. Using some initial simple examples, we provided a clear exhibition of the advantages of the proposed scheme. Note that such a scheme can enable information sharing under a relatively low SNR (say less than −8dB), using the specific *signal structure* in frequency domain. As the implementation of the scheme is easy at PU, PU's some other important status information can also be shared in this way without squander its time-domain resource. Hence the scheme will potentially be meaningful directions for further research.

References

1. Liang, Y.-C., Chen, K.-C., et al.: Cognitive radio networking and communications: An overview. IEEE Trans. Veh. Technol. **60**(7), 3386–3407 (2011)
2. Alasti, M., Neekzad, B., Hui, J., Vannithamby, R.: Quality of service in WiMAX and LTE networks. IEEE Commun. Mag. **48**(5), 104–111 (2010)
3. Hoang, A.T., Liang, Y.-C., Islam, M.H.: Maximizing throughput of cognitive radio networks with limited primary users' cooperation. In: Proc. IEEE ICC (2007)
4. Zhang, W., Yeo, C.K., Li, Y.: A MAC sensing protocol design for data transmission with more protection to primary users. IEEE Trans. Mobile Comput. **12**(4), 621–632 (2013)
5. Hoang, A.T., Liang, Y.-C., Islam, M.H.: Power control and channel allocation in cognitive radio networks with primary users' cooperation. IEEE Trans. Mobile Comput. **9**(3), 348–360 (2010)
6. Mahmoud, H.A., Yücek, T., Arslan, H.: OFDM for cognitive radio: merits and challenges. IEEE Wireless Commun. Mag. **16**(2), 6–15 (2009)
7. Liang, Y.-C., Zeng, Y., et al.: Sensing-throughput tradeoff for cognitive radio networks. IEEE Trans. Wireless Commun. **7**(4), 1326–1337 (2008)
8. IEEE 802.16 Working Group. IEEE Standard for Local and Metropolitan Area Networks, Part 16: Air Interface for Fixed Broadband Wireless Access Systems Amendment3: Advanced Air Interface, IEEE Std, vol. 802 (2011)
9. IEEE 802.11-2007: Wireless LAN medium access control (MAC) and physical layer (PHY) specifications, IEEE 802.11 LAN Standards (2007)
10. López-Benıtez, M., Casadevall, F.: Time-dimension models of spectrum usage for the analysis, design and simulation of cognitive radio networks. IEEE Trans. Veh. Technol. **62**(5), 2091–2104 (2013)